Standardized Centralized Alzheimer's and Related Dementias Neuroimaging (SCAN)

MRI Analysis Methods Manual

Document Status:	Final
Document Revision Number:	1.0
Date:	19 September 2023

Contents

1. Contact Information for the SCAN Study 3
2. Background and Significance of MRI in the SCAN Study 3
3. MRI Human Scan Protocol 3
4. Quality Control 4
5. Clinical Review/Alerts 4
6. Analysis Procedures 4
6.1. Structural MRI 4
6.2. T2 GRE 4
6.2.1. Cerebral Micro Bleed (CMB) 4
6.2.2. Quantitative Susceptibility Mapping (QSM) 5
6.3. 3D pCASL or 3D PASL 6
6.3.1. Arterial Spin Labeling (ASL) Perfusion Values 6
6.4. Diffusion Imaging 7
6.4.1. Mean Diffusivity (MD) and Fractional Anisotropy (FA) 7
6.4.2. Neurite Orientation Dispersion and Diffusion Imaging (NODDI) 8
6.5. fMRI 8
6.5.1. Network Failure Quotient (NFQ) 8
7. Deliverables 8
8. References 8

1. CONTACT INFORMATION FOR THE SCAN STUDY

If you have any questions or concerns regarding MRI imaging, please contact the Mayo Clinic Aging and Dementia Imaging Research (ADIR) Laboratory:

SCANMRI@mayo.edu

If you have any questions regarding the scan uploading or downloading, please contact LONI:

dba@loni.usc.edu

2. BACKGROUND AND SIGNIFICANCE OF MRI IN THE SCAN STUDY

https://scan.naccdata.org/

The goal of SCAN will be to promote standardization of PET and MR image acquisition so that images can be combined across multiple centers. Moreover, SCAN imaging methods are intentionally matched to ADNI4 with the specific goal of being able to combine SCAN and ADNI4 data for analyses. The prospectively acquired SCAN images will be subject to standardized quality control procedures, appropriately archived, labeled, and made available to qualified investigators on the LONI website. In addition, the SCAN team will develop numeric summaries of the PET and MR data that will be available on the LONI website and linked to the ADRC participants through their NACC ID. Appropriate images for inclusion in the SCAN workflow are images acquired prospectively on NACC participants, following SCAN protocols regardless of the funding source.

SCAN has a set of required acquisition schemes for MR data that are identical to ADNI4. This includes, at minimum, SCAN MRI sequences for structural T1 and FLAIR scans. Additional, MR sequences using the prescribed SCAN protocol parameters may be acquired, but these are optional. Analyzed MRI data available to investigators will include regional measures of brain volume, white matter hyperintensities, cerebral infarction, and, depending on the availability of additional MR sequences, diffusion MR parameters, cerebral blood flow, microbleeds, regional susceptibility, dilated perivascular spaces and functional connectivity.

3. MRI HUMAN SCAN PROTOCOL

There are two MR protocol options for SCAN – each site can choose which they prefer:

Option 1: MRI site only required to do two SCAN sequences:
1. Sagittal 3D Accelerated MPRAGE/IRSPGR (ADNI4 Sequence)
2. Sagittal 3D FLAIR (ADNI4 Sequence)

Option 2: MRI site performs the full SCAN protocol (ADNI4)
1. 3 Plane/Tri-Planar Scout/Calibration Scan
2. Sagittal 3D Accelerated MPRAGE/IRSPGR
3. Sagittal 3D FLAIR
4. Sagittal 3D T2 Space
5. Axial 3D ME T2 GRE / Axial 3D T2 GRE / Axial T2 Star/GRE

6. Axial DTI PA (Multiband if applicable)
7. Axial DTI AP (Philips and Siemens only, multiband if applicable)
8. Axial fcMRI (Participant should have eyes OPEN) - (Multiband if applicable)
9. Axial 3D pCASL / Axial 3D PASL
10. Accelerated High Resolution Hippocampus Scan (Oblique – perpendicular to hippocampal tail)

Except for the HRHippocampal sequence, all scans should be scanned as straight axial or sagittal.

4. QUALITY CONTROL

Each series in each exam undergoes quality control at Mayo Clinic ADIR Lab. Two levels of quality control are performed: adherence to the protocol parameters and series specific quality (i.e., participant motion, anatomic coverage, etc). Scan quality is graded subjectively by trained image analysts: a rating of 1-3 is acceptable and 4 is failure (unusable). This QC information will be available for each series on LONI. Thus, users will be able to employ series level QC information as filters in data collections.

5. CLINICAL REVIEW/ALERTS

Review of scans were performed at each field center to screen for clinically significant abnormalities (e.g., acute hemorrhage and/or mass effect). In addition, the ADIR Lab also assessed all incoming scans for medically significant abnormalities, and notified the data center if a significant abnormality was identified. The central read (Mayo) information on clinically relevant abnormalities will go into the SCAN data base.

6. ANALYSIS PROCEDURES

6.1. Structural MRI

Charles DeCarli's UCD lab will provide numeric values of ROI-level cortical thickness.

Charles DeCarli's UCD lab will provide cerebrovascular disease metrics of white matter hyperintensity volume and brain infarctions.

6.2. T2 GRE

6.2.1. Cerebral Micro Bleed (CMB)

If a site includes the SCAN GRE sequence in the SCAN acquisition, then the ADIR Lab will provide data on number and location of all cerebral micro bleeds and superficial siderosis.

Cerebral micro bleeds and areas of superficial siderosis are enumerated and anatomically localized by trained image analysts and confirmed by neuroradiologists. For each image used in CMB assessment, the T1-weighted image within the same imaging study is used to provide information about the anatomic location of finding. The T1 image carries with it 22 region anatomic labeling atlas as well as maps of the probability of the participant gray matter, white matter, and CSF (Figure 1). For each

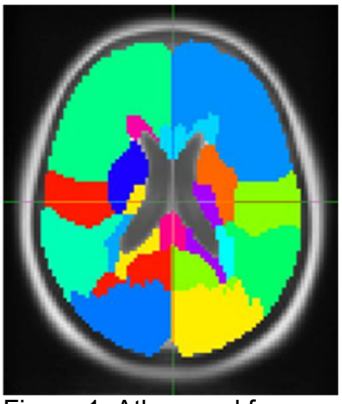

Figure 1. Atlas used for CMB assessment.

finding, the gray matter, white matter and CSF probabilities at the location of the finding are included. Regions include the following 22 areas:
01 PV_front_L
02 PV_front_R
03 deep_gray_and_white_L
04 deep_gray_and_white_R
05 anterior_corpus_callosum
06 posterior_corpus_callosum
07 SC_temp_L
08 SC_temp_R
09 SC_front_L
10 SC_front_R
11 SC_occip_L
12 SC_occip_R
13 PV_occip_L
14 PV_temp_L
15 PV_temp_R
16 PV_occip_R
17 SC_pariet_R
18 SC_pariet_L
19 PV_pariet_L
20 PV_pariet_R
21 brainstem
22 cerebellum

6.2.2. Quantitative Susceptibility Mapping (QSM)

If a site includes the SCAN ME (multi echo) GRE sequence in the SCAN acquisition, then ROI-level QSM values will be provided by the ADIR Lab. Quantitative susceptibility mapping (QSM) is a magnetic resonance imaging (MRI) technique that estimates the local intrinsic magnetic susceptibility of tissues. We use a multi-echo gradient recall echo (GRE) MRI acquisition to acquire the images necessary to make these estimates. Quantitative susceptibility mapping using a multi-echo GRE MRI acquisition has been shown to help differentiate paramagnetic susceptibility (iron deposits) from diamagnetic susceptibility (calcifications), which is often challenging to do with susceptibility-weighted imaging (SWI). Therefore, QSM processing on multi-echo GRE MRI enables 3D estimation of iron deposits throughout the brain. As is true elsewhere in this document, text in the following paragraphs can be used to describe SCAN QSM processing methods for manuscripts.

We use multi-echo GRE MRI product sequences that are able to output full complex data (either magnitude and phase or real and imaginary), to acquire five brain volumes at five separate echo times, with separate images saved for phase and magnitude. For anatomical segmentation and labeling, we use the high-resolution T1-weighted magnetization-prepared rapid acquisition gradient echo (MPRAGE) acquisition for each participant.

For each participant visit with both a useable T1 MPRAGE and multi-echo GRE MRI, we first generate gray matter, white matter and cerebrospinal fluid tissue class volumes, and an inhomogeneity corrected version of the T1 volume, using SPM12 unified segmentation[1] with custom tissue priors from the Mayo Clinic Adult Lifespan Template

(MCALT)[2]. We combine the participant space segmentations to generate a total intracranial volume mask, and use ANTs non-linear registration[3] to register region of interest (ROI) masks from the MCALT space to participant T1 space. We use SPM12 rigid registration to compute an affine transformation between the first echo of the GRE magnitude image and the T1 MPRAGE, then apply the series of transformations to propagate the TIV mask and ROIs from MCALT space into GRE space.

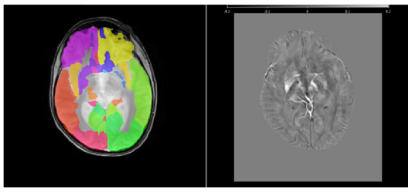

Figure 2: Example case showing the first echo of the GRE magnitude image with ROIs overlaid (left), and the corresponding QSM image (right).

We used components from STI Suite software[4] to build a fully automated pipeline to compute the QSM image from the multi-echo GRE MRI for each participant. Briefly, the steps we use are as follows: first, we first apply a Laplacian-based phase unwrapping[5] to unwrap the phase from each echo; next, we sum the resulting unwrapped phase images across all three echo times, to form an unwrapped summed phase image and we then apply V-SHARP[6] filtering to remove the bias field, using the TIV mask to restrict the impact of noise from outside the TIV on upstream QSM processing; finally, we compute the QSM image on the bias corrected unwrapped phase image, using the iterative least squares (iLSQR) method[7]. After these steps, we apply the ROI masks propagated from the participant's T1 image to obtain median magnetic susceptibility values from each ROI in the atlas, as depicted in Figure 2.

6.3. 3D pCASL or 3D PASL

6.3.1. Arterial Spin Labeling (ASL) Perfusion Values

If a site includes the SCAN 3D pCASL or 3D PASL sequence in the SCAN acquisition, then ROI-level relative perfusion values will be provided by the ADIR Lab. Arterial Spin Labeling (ASL) is a magnetic resonance imaging (MRI) technique that facilitates estimation of the perfusion of blood into the brain. Depending on the site-specific MRI manufacturer and model, we acquire either a multiple label delay 3D Pulsatile Arterial Spin Labeling (MLD-PASL), or a multiple label delay 3D pseudo-continuous ASL (MLD-pCASL) multiple Pulse Label Delay. The multiple labeling delays allow for robust estimates of cerebral blood flow (CBF) and arterial transit time (ATT) on a 3D voxel-wise basis throughout the brain. As is true elsewhere in this document, text in the following paragraphs can be used to describe SCAN QSM processing methods for manuscripts.

We use MLD-PASL and MLD-pCASL MRI product sequences that output either a sequence of control and labelled images for each label delay time, typically repeated four times for each label delay in the case of MLD-PASL; or a series of M0 images and difference images representing tagged minus control for each label delay time in the case of MLD-pCASL. For anatomical segmentation and region of interest (ROI) quantification, we use the high-resolution T1-weighted magnetization-prepared rapid acquisition gradient echo (MPRAGE) acquisition for each participant.

For each participant visit with both a useable T1 MPRAGE and MLD-PASL or MLD-pCASL MRI, we first generate gray matter, white matter, and cerebrospinal fluid tissue class volumes, and an inhomogeneity corrected version of the T1 volume, using SPM12 unified segmentation[1] with custom tissue priors from the Mayo Clinic Adult Lifespan

Template (MCALT)[2]. We combine the participant space segmentations to generate a total intracranial volume mask and used ANTs non-linear registration[3] to register region of interest (ROI) masks from the MCALT space to participant T1 space. We use SPM12 rigid registration to compute an affine transformation between the mean of the ASL control images in the case of PASL or mean M0 in the case of pCASL, and the T1 MPRAGE, then apply the series of transformations to propagate the TIV mask and ROIs from MCALT space into ASL space.

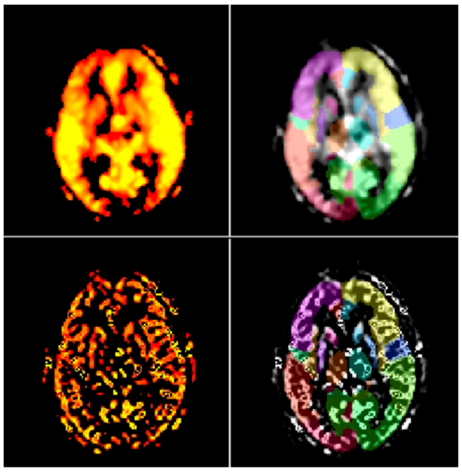

Figure 3. Top row: Example CBF map from a SIEMENS 3D MLD-PASL (top left); CBF map with atlas ROIs overlaid (top right). Bottom row: Corresponding ATT map (bottom left), and ATT map with atlas ROIs overlaid (bottom right).

We used components from SPM12 and FSL BASIL software[8, 9] to build a fully automated pipeline to compute the CBF and ATT images from the MLD-PASL or MLD-pCASL MRI for each participant. Briefly, the steps we used are as follows: first, we used dcm2niix software to convert the DICOM to NIfTI format. In some cases, the multiple label delays result in separated DICOM series for each label delay. We next extract the bolus duration and label delay times from the DICOM headers and combine the multiple series into a single 4D NIfTI file. Then, we use the command line tool, oxford_asl, from the FSL BASIL toolbox, to calculate CBF and ATT maps for the input MLD-PASL or MLD-pCASL. After these steps, we finally apply the ROI masks propagated from the participant's T1 image to obtain mean or median CBF and ATT values from each ROI in the atlas, as depicted in Figure 3.

6.4. Diffusion Imaging

6.4.1. Mean Diffusivity (MD) and Fractional Anisotropy (FA)

If a site includes the SCAN diffusion sequence in the SCAN acquisition, then ROI-level diffusion values will be provided by the ADIR Lab. Mean diffusivity (MD) and fractional anisotropy (FA) maps are created by fitting tensors to the diffusion values using a non-linear least squares algorithm after denoising and correcting for head motion, eddy current distortion, Gibbs ringing, and Rician bias. ROI-wise median MD and FA values are derived using the Johns Hopkins University (JHU) single participant "Eve" atlas[10] after warping it to each scan's native space using non-linear FA to FA registration. Voxels with MD > 0.002 mm^2/s are excluded from the atlas since they are mostly CSF, and the median voxel value within each ROI is reported, since the mean is more vulnerable to contamination by partial volume effects in each ROI's edge voxels. Missing values for an ROI indicate that no voxels were assigned to it, due to scan coverage, resolution, artifacts, or participant anatomical differences in that atlas region.

The atlas has been modified slightly by combining the left and right portions of structures spanning the medial plane, such as the corpus callosum and pons. Being based on a single person, the "Eve" atlas is somewhat asymmetric, so any apparent left-right differences found using it should be treated with caution. A simplified version of the table

is also available, with the number of atlas regions pared down to the genu of the corpus callosum (GCC) and the average of the left and right hippocampal cingulum (CGH) values, weighted by the number of voxels in the left and right portions. The GCC is the best region for examining cerebrovascular issues, and the CGH is ideal for non-vascular issues.

6.4.2. Neurite Orientation Dispersion and Diffusion Imaging (NODDI)

For exams that use the multi-shell diffusion MR acquisition, the ADIR Lab will provide ROI values for the Neurite Density Index, Orientation Dispersion Index, and Isotropic (Free Water) Volume Fraction from NODDI, using the JHU “Eve” atlas and another one more suitable for gray matter (to be determined). Since NODDI explicitly models multiple components in each voxel, all of the NODDI values are provided for both gray and white matter.

6.5. fMRI

6.5.1. Network Failure Quotient (NFQ)

If a site includes the SCAN resting fMRI sequence in the SCAN acquisition, then NFQ values will be provided by the ADIR Lab. The Network Failure Quotient (NFQ) is described in Wiepert et. al.[11]. Briefly, higher scores are correlated with more advanced cognitive decline.

Results provided include the connectivity estimates used in calculating the NFQ, the NFQ value, and a single overall quality control estimate.

Additionally, the timing of the acquired images is provided as list of underscore separated values. The timing information is believed to be accurate but not guaranteed as some MRI vendors do not capture detailed timing information well in DICOM formatted image data. Timing values for slices in a single volume are included where the slice ordering is reckoned inferior to superior regardless of the slice ordering in DICOM data.

7. DELIVERABLES

The ADIR Lab sends the data to LONI on a quarterly basis.

8. REFERENCES

1. Ashburner, J. and K.J. Friston, Unified segmentation. NeuroImage, 2005. 26(3): p. 839-51. Available from: http://www.ncbi.nlm.nih.gov/pubmed/15955494.
2. Schwarz, C.G., J.L. Gunter, C.P. Ward, P. Vemuri, M.L. Senjem, H.J. Wiste, R.C. Petersen, D.S. Knopman, and C.R. Jack, The Mayo Clinic Adult Lifespan Template: Better Quantification Across the Lifespan. Alzheimer's & Dementia, 2017. 13(7): p. 2. Available from: https://www.sciencedirect.com/science/article/pii/S1552526017313043.
3. Avants, B.B., C.L. Epstein, M. Grossman, and J.C. Gee, Symmetric diffeomorphic image registration with cross-correlation: evaluating automated labeling of elderly and neurodegenerative brain. Medical image analysis, 2008. 12(1): p. 26-41. Available from: http://www.ncbi.nlm.nih.gov/pubmed/17659998.
4. Schofield, M.A. and Y. Zhu, Fast phase unwrapping algorithm for interferometric applications. Opt Lett, 2003. 28(14): p. 1194-6. Available from: https://www.ncbi.nlm.nih.gov/pubmed/12885018.

5. Liu, C., STI Suite. Available from: https://people.eecs.berkeley.edu/~chunlei.liu/software.html.
6. Wu, B., W. Li, A. Guidon, and C. Liu, Whole brain susceptibility mapping using compressed sensing. Magn Reson Med, 2012. 67(1): p. 137-47. Available from: https://www.ncbi.nlm.nih.gov/pubmed/21671269.
7. Li, W., B. Wu, and C. Liu, Quantitative susceptibility mapping of human brain reflects spatial variation in tissue composition. Neuroimage, 2011. 55(4): p. 1645-56. Available from: https://www.ncbi.nlm.nih.gov/pubmed/21224002.
8. Chappell, M., G. AR, W. B, and W. MW, Variational Bayesian inference for a non-linear forward model. IEEE Transactions on Signal Processing, 2009. 57(1): p. 223-236.
9. Chappell, M.A., B.J. MacIntosh, M.J. Donahue, M. Gunther, P. Jezzard, and M.W. Woolrich, Separation of macrovascular signal in multi-inversion time arterial spin labelling MRI. Magnetic Resonance in Medicine, 2010. 63(5): p. 1357-1365. Available from: https://onlinelibrary.wiley.com/doi/10.1002/mrm.22320.
10. Oishi, K., A. Faria, H. Jiang, X. Li, K. Akhter, J. Zhang, J.T. Hsu, M.I. Miller, P.C. van Zijl, M. Albert, C.G. Lyketsos, R. Woods, A.W. Toga, G.B. Pike, P. Rosa-Neto, A. Evans, J. Mazziotta, and S. Mori, Atlas-based whole brain white matter analysis using large deformation diffeomorphic metric mapping: application to normal elderly and Alzheimer's disease participants. Neuroimage, 2009. 46(2): p. 486-99. Available from: https://www.ncbi.nlm.nih.gov/pubmed/19385016.
11. Wiepert, D.A., V.J. Lowe, D.S. Knopman, B.F. Boeve, J. Graff-Radford, R.C. Petersen, C.R. Jack, Jr., and D.T. Jones, A robust biomarker of large-scale network failure in Alzheimer's disease. Alzheimers Dement (Amst), 2017. 6: p. 152-161. Available from: https://www.ncbi.nlm.nih.gov/pubmed/28275697.